Determination of the surface and interface phase shifts in metallic quantum well structures of perovskite oxides

K. Yoshimatsu,[1,2] E. Sakai,[1] M. Kobayashi,[1] K. Horiba,[1] T. Yoshida,[2] A. Fujimori,[2] M. Oshima,[3,4] and H. Kumigashira[1,5,*]

[1]*Photon Factory, Institute of Materials Structure Science, High Energy Accelerator Research Organization (KEK), 1-1 Oho, Tsukuba 305-0801, Japan*

[2]*Department of Physics, University of Tokyo, 7-3-1 Hongo, Bunkyo-ku, Tokyo 113-0033, Japan*

[3]*Department of Applied Chemistry, University of Tokyo, 7-3-1 Hongo, Bunkyo-ku, Tokyo 113-8656, Japan*

[4]*Synchrotron Radiation Research Organization, The University of Tokyo, Bunkyo-ku, Tokyo 113-8656, Japan*

[5]*PRESTO, Japan Science and Technology Agency, Kawaguchi, Saitama 332-0012, Japan*

(Received 17 June 2013; revised manuscript received 1 September 2013; published 19 September 2013)

We propose an experimental approach to extract separately the surface and interface phase shift of standing waves in metallic quantum well (QW) structures composed of isostructural perovskite oxides. The "asymmetric" vacuum/$SrVO_3$/$SrTiO_3$ and "symmetric" $SrTiO_3$/$SrVO_3$/$SrTiO_3$ QW structures are fabricated in an epitaxial multilayer form. Using these metallic QW structures, the phase shifts at the surface (vacuum/$SrVO_3$) and interface ($SrTiO_3$/$SrVO_3$) are successfully obtained by analyzing a thickness series of angle-resolved photoemission spectra. The difference of the phase shift between the two boundaries reveals that nearly ideal quantum confinement is achieved at the interface, indicating that a $SrTiO_3$ layer acts as a useful potential barrier.

DOI: 10.1103/PhysRevB.88.115308 PACS number(s): 73.21.Fg, 73.20.−r, 79.60.−i, 71.27.+a

I. INTRODUCTION

Quantum well (QW) states have been a great contribution to the development of both fundamental physics and electric devices used for modern information technology.[1–12] Recently, QW states were clearly observed for strongly correlated oxides by means of angle-resolved photoemission spectroscopy (ARPES): $SrVO_3$ (SVO) ultrathin films[13] as well as cleaved $SrTiO_3$ (STO) and $KTaO_3$ surfaces.[14–16] Such QW structures are relevant to understanding two-dimensional quantum confinement (phenomena) in strongly correlated oxides, which have attracted considerable attention for their potential use in the control of the novel functionalities of strongly correlated oxides using artificial structures.[17,18]

In order to design the functionalities of the oxide QW structures, it is desirable to obtain knowledge of the complex interactions of the confined strongly correlated electrons at the boundaries, especially the phase shift (reflection) of the electron at the surface and the interface. However, unfortunately, the phase shifts at the two boundaries cannot be extracted separately because one obtains the information as a "total phase shift" term of Φ, which is defined as the sum of the phase shifts at the surface and the interface in the quantization condition for a numerical formula.[1–12] Therefore, the phase shifts at the two boundaries have been treated as the fitting parameters to describe the QW states[1–4] or estimated with the help of theoretical calculations,[10,11] although the phase shift is an essential term to discuss the confinement condition in the metallic QW structures.

In this article, we propose a method of analysis to experimentally determine the phase shifts at the two boundaries using the "asymmetric and symmetric" QW structures. These QW structures consist of isostructural perovskite oxides with a chemical formula of ABO_3. The symmetric $A'B'O_3$/ABO_3/$A'B'O_3$ QW structures, where electrons are geometrically confined inside the ABO_3 layers, have the same boundaries of the ABO_3/$A'B'O_3$ interfaces. Thus the total phase shift of this symmetric QW structure is twice the phase shift at the ABO_3/$A'B'O_3$ interface. Meanwhile, the total phase shift of the asymmetric QW structure (vacuum/ABO_3/$A'B'O_3$) is obtained as the sum of the phase shifts at the ABO_3 surface and the ABO_3/$A'B'O_3$ interface. As a result, the phase shifts at the surface and the interface are separately determined by solving simple simultaneous equations without any help from theoretical calculations.

Using the metallic QW structures composed of the conductive oxide SVO and the oxide semiconductor STO, we successfully determined the phase shift at the surface (vacuum/SVO) and the interface (STO/SVO) by analyzing an SVO-layer thickness series of ARPES spectra. The difference in the phase shift between the two boundaries reveals that the nearly perfect reflection of standing waves is achieved at the STO/SVO interface owing to the high permittivity of STO and its band lineup to SVO. These results have a significant implication for designing oxide QW structures. In addition, the successful determination suggests that our analytical approach permits direct access to the behavior of confined electrons and will be widely applicable to the studies of QW structures.

II. EXPERIMENT

Digitally controlled SVO ultrathin films (asymmetric QW structures) were grown on atomically flat TiO_2-terminated Nb-doped STO substrates by a pulsed laser deposition method. Details of the growth conditions are described elsewhere.[19] For fabricating STO/SVO/STO (symmetric QW) structures, one monolayer of STO was subsequently deposited onto the SVO ultrathin films in the same growth conditions. In order to eliminate the possibility that changes in the composition might cause the difference in the QW states between the asymmetric and symmetric QW structures, both the QW structures were fabricated at the same time on the same STO substrate. The thicknesses of SVO films and STO overlayers were controlled

by monitoring the intensity oscillation of the specular spot of the reflection high-energy electron diffraction.

The ARPES measurements were performed *in situ* at BL28A of Photon Factory, KEK. The energy resolution was set to 30 meV at a photon energy of 88 eV. All the ARPES measurements were performed at 20 K using linearly polarized light. The Fermi level (E_F) of the samples was referred to that of a gold foil. Detailed ARPES measurement conditions are described elsewhere.[13]

III. RESULTS AND DISCUSSION

Figure 1 shows the ARPES spectra taken at the Γ point as a function of SVO film thickness with and without an STO overlayer. The former corresponds to the symmetric QW structure of STO/SVO/STO, whereas the latter is the asymmetric QW structure of vacuum/SVO/STO. Regardless of the presence or absence of the STO overlayer, several peaks derived from the QW states were clearly observed in the ARPES spectra. Because STO is an *n*-type semiconductor with a band gap of 3.2 eV, an STO overlayer does not mask the QW states derived from the V 3*d* states of the buried SVO layers. Thus we address the buried QW states by ARPES. At first glance, there seems to be no significant change in both the ARPES spectra; the spectral line shapes

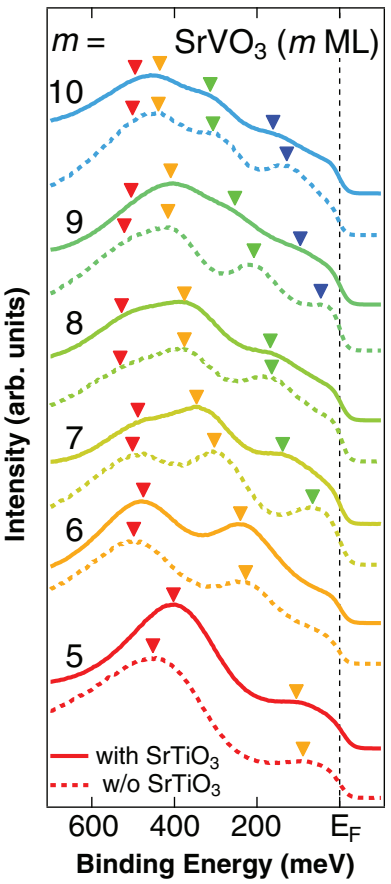

FIG. 1. (Color online) Thickness-dependent ARPES spectra of $SrVO_3$ ultrathin films taken at the Γ point with (solid lines) and without (dashed lines) a $SrTiO_3$ overlayer. The filled triangles indicate the peak positions in the ARPES spectra.

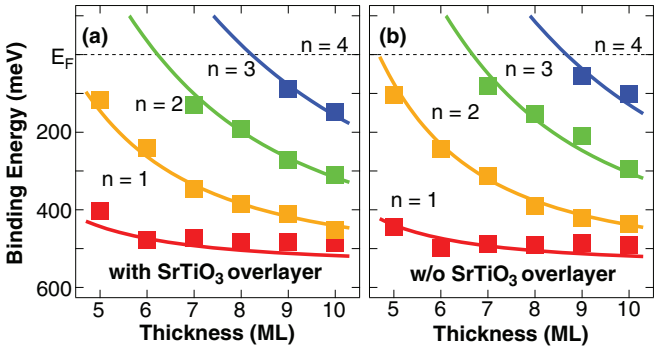

FIG. 2. (Color online) Structure plot of $SrVO_3$ ultrathin films (a) with and (b) without a $SrTiO_3$ overlayer. The marker colors correspond to those of the triangles in Fig. 1. The markers and solid lines are the experimental data and simulated results based on the phase shift quantization rule (see text for details), respectively.

are similar to each other, and the number of the peaks is the same in the ARPES spectra for the same SVO film thickness. However, a closer look reveals that the peak positions of the quantized states show slight differences between the two QW structures. The quantized states located in the vicinity of E_F are slightly shifted toward a higher binding energy in the "symmetric" QW structure of STO/SVO/STO, whereas the quantized states near the bottom of the V 3*d* conduction bands [∼500 meV (Refs. 20–22)] shift in the opposite direction. It should be noted that these behaviors cannot be explained by the chemical potential shift and/or charge transfer derived from the additional STO overlayer because all the peaks should be shifted toward the same energy direction in such a case.

In order to investigate the differences in the quantized states between the two kinds of QW structures more clearly, we plot the peak positions as a function of SVO film thickness in Fig. 2. For both of the QW structures, the quantized states are finally saturated at the binding energy of ∼500 meV, where the bottom of the bulk V 3*d* conduction bands in SVO is located.[20–22] As expected from Fig. 1, the quantized states located in the lower binding energy region exhibit differences in their peak positions between the two QW structures. Considering the structural difference in these QW structures, the differences in peak positions should reflect the degree of the quantum confinement at the surface and the interface, which is represented by the total phase shift in the phase shift quantization rule.[1,2]

In order to estimate the total phase shifts for both of the QW structures, we simulated the structure plots by only changing the total phase shift, while other parameters were fixed. In the phase shift quantization rule, the quantization condition is described by the following equation:[12]

$$2k_{\mathrm{env}}L + \Phi = 2n\pi, \qquad (1)$$

where k_{env}, L, Φ, and n are the wave vector of the envelope function, the width of the QW, the total phase shift, and the quantum number, respectively. In this analysis, we define quantum number n as starting from 1. Here, L is defined as $L = ma$, where m is the number of monolayers for SVO ultrathin films ($m = 1, 2, \ldots$) and a is the out-of-plane lattice constant of SVO thin films. The details of the simulation based on the phase shift quantization rule and the renormalization scheme of

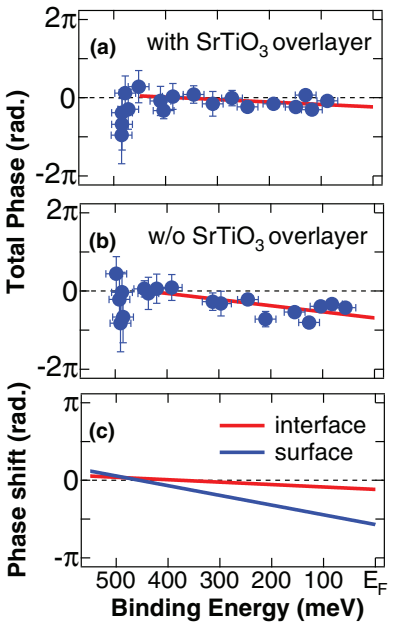

FIG. 3. (Color online) Plots of the total phase shift of the metallic quantum well states in $SrVO_3$ layers (a) with and (b) without a $SrTiO_3$ overlayer as a function of binding energy. The markers with error bars denote the total phase shift obtained from analyzing the experimental data (see text for details). The solid lines are the results of the least-squares linear fitting for the data. (c) The phase shift at the $SrVO_3$ surface and the $SrTiO_3/SrVO_3$ interface.

the tight-binding calculation are described elsewhere.[13] These results are superimposed on solid lines in Figs. 2(a) and 2(b) for the symmetric and asymmetric QW structures, respectively. The simulated results reproduce the experimental results well, confirming that these observed states are derived from the quantized states in SVO layers in the metallic QW structures.

Figures 3(a) and 3(b) show the evaluated energy dependence of the total phase shifts in both QW structures. The experimentally obtained total phase shifts are well fitted by a least-square regression line[9,23] as indicated by the solid lines in Figs. 3(a) and 3(b). The fitted total phase shifts show a qualitatively similar binding-energy dependence between the two. As shown by extrapolating the fitted lines toward higher binding energies, the experimental phase shift is almost zero at the bottom energy of the V $3d$ conduction bands in bulk SVO ($\sim$ 500 meV). On the other hand, the slopes of the total phase shifts as a function of binding energy are considerably different between the two QW structures.

The difference in the total phase shift is responsible for the modulation of the wave function in the QW at the boundaries. For an examination of the behavior of the standing waves at the boundaries of the SVO layers, we extracted the phase shifts at the surface and interface separately as follows. In Eq. (1), the total phase shift in the present STO/SVO/STO QW structures is written as $\Phi_{sym} = \Phi_{interf} + \Phi'_{interf}$. Meanwhile, in the vacuum/SVO/STO QW structures, the total phase shift is $\Phi_{asym} = \Phi_{surf} + \Phi_{interf}$. Here, Φ_{interf}, Φ'_{interf}, and Φ_{surf} are the phase shifts at the SVO/STO substrate interface, SVO/STO overlayer interface, and SVO surface, respectively. Assuming $\Phi_{interf} \approx \Phi'_{interf}$, the phase shift at the surface and the interface could be obtained separately by solving the simple simultaneous equations. Although the STO overlayer is very thin, the assumption may serve as a good approximation in the present case. As can be observed in Figs. 3(a) and 3(b), the absolute value of Φ_{sym} is close to zero and considerably smaller than that of Φ_{asym}, strongly suggesting that the absolute value of Φ_{interf} as well as Φ'_{interf} is almost zero and they are quite smaller than that of Φ_{surf}.

The separate phase shifts are shown in Fig. 3(c). As expected from the difference of total phase shifts in Figs. 3(a) and 3(b), the phase shift at the interface is almost independent of the binding energy and close to zero. On the contrary, the phase shift at the surface strongly depends on binding energy, and its absolute value is considerably higher than that at the interface from 500 meV to E_F where the QW states were observed from the ARPES spectra.

Next, we discuss the relationship between the phase shift and the behaviors of the standing waves at the boundaries. Considering the special case in which the total phase shift is zero ($\Phi_{surf} = \Phi_{interf} = 0$), $k_{env} = \pi/a$ is one solution of Eq. (1) for all $m = n$. This means that the wave functions of the standing waves have zero amplitude at the boundaries.[2,9] In contrast, when the total phase shift is almost 2π ($\Phi_{surf} = \Phi_{interf} \approx \pi$), there are no solutions for $n = 1$ (the only answer is $k_{env} = 0$).[2] In other words, the standing waves are better confined inside the QW when the phase shift is close to zero.

Based on this relationship, we will compare the phase shift between the two boundaries. Both the phase shifts are almost zero at 500 meV, indicating that ideal quantum confinement is achieved around this energy range. With decreasing binding energy, both the phase shifts deviate from zero, suggesting that the standing waves somewhat penetrate into the potential barriers. The phase shift at the surface is farther from zero

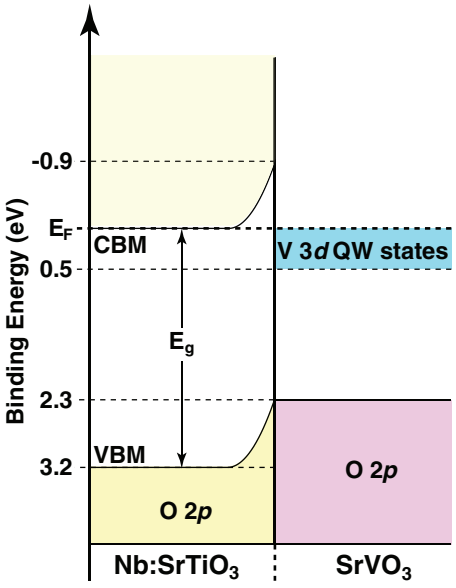

FIG. 4. (Color online) Band diagram of the $SrTiO_3/SrVO_3$ interface deduced from the previous PES studies.[13,24,25] CBM and VBM denote the conduction band minimum and valence band maximum, respectively. The V $3d$ conduction bands are energetically well isolated from both the CBM and VBM owing to the wide band gap of $SrTiO_3$ and its band lineup to $SrVO_3$.

than that at the interface, indicating that the standing waves are considerably better confined at the interface than at the surface. This result suggests that the interfaces with STO as well as STO overlayer are useful for the quantum confinement of the V 3*d* states in SVO.

Finally, we briefly discuss the reason why an STO layer acts as nearly ideal potential barriers in terms of the band diagram at the SVO/STO interface. The band diagrams drawn from the previous photoemission studies[13,24,25] are illustrated in Fig. 4. At the interface between the metallic SVO and the *n*-type semiconductor STO, a Schottky potential barrier of 0.9 eV is formed.[13] Because STO has a wide band gap of 3.2 eV, the occupied V 3*d* states involved in the formation of the observed QW states in the energy range from E_F to 0.5 eV are located around the middle of the band gap of STO. Namely, the occupied QW states are energetically well isolated from the conduction band minimum (offset of ∼0.9 eV) and valence band maximum (offset of ∼1.8 eV) of STO at the interface. In such circumstances, it is difficult for an electron in the SVO layer to couple to any electronic states in STO. It should be noted that the valence band maximum of the STO overlayer is located around 2.3 eV (not shown), strongly suggesting the formation of almost the same band lineup between the upper and lower interfaces. This fact provides further support for the validity of our analysis based on the assumption of $\Phi_{\mathrm{interf}} \approx \Phi'_{\mathrm{interf}}$ and may be responsible for the formation of better quantum confinement of V 3*d* electrons in the symmetric QW structures.

Considering the band lineup at the SVO/STO interface in Fig. 4, the STO layers are regarded as a "vacuum" with higher permittivity for the V 3*d* electrons at a first approximation. STO is a quantum paraelectric material and its relative permittivity at the present measurement temperature of 20 K is more than 10 000,[26] although the value may degrade in thin film form and/or crystal deformation in the interfacial region.[27,28] In such a high value of permittivity, the barrier-energy lowering near the interface due to the image force (image-force lowering known as the Schottky effect)[29] is negligibly weak, and the shape of energy potential near the interface approaches asymptotically to the intrinsic Schottky barrier as shown in Fig. 4. In other words, the abrupt potential well is formed at the interface, and consequently nearly ideal quantum confinement of V 3*d* electrons could be achieved. These results have an important implication for designing oxide QW structures; other oxide semiconductors with a wide band gap and a high permittivity are used as nearly ideal potential barriers to confine electrons in oxide heterostructures. In order to test this capability, further systematic investigation, as well as theoretical studies, is necessary.

IV. CONCLUSION

We have experimentally determined the phase shifts of the standing waves in SVO at the surface (vacuum/SVO) and the interface (STO/SVO) separately by using the symmetric and asymmetric QW structures. By analyzing a thickness series of ARPES data, it has been found that the V 3*d* states are well confined at the two boundaries. The obtained phase shifts suggest that nearly ideal quantum confinement is achieved at the STO/SVO interfaces owing to the wide band gap and high permittivity of STO and its band lineup to SVO. These results strongly suggest that the metallic QW states of strongly correlated electrons are created by using the combination of the conductive oxides and oxide semiconductors with a wide gap and a high permittivity, and designed by tuning the band lineup among them. Furthermore, this structural design concept can be generalized to create the metallic QW states in other systems.

ACKNOWLEDGMENTS

The authors are very grateful to I. Matsuda and F. Komori for useful discussions. This work was supported by a Grant-in-Aid for Scientific Research (B25287095 and S22224005) and Research Activity Start-up (25887021) from the Japan Society for the Promotion of Science (JSPS), the JST PRESTO program, and MEXT Element Strategy Initiative to Form Core Research Center. K.Y. acknowledges the financial support from JSPS for Young Scientists. The work at KEK-PF was performed under the approval of the Program Advisory Committee (proposals 08S2-003, 09S2-005, 11S2-003, 2012G075, 2012G536, and 2012G688) at the Institute of Materials Structure Science, KEK.

*hiroshi.kumigashira@kek.jp

[1] T.-C. Chiang, Surf. Sci. Rep. **39**, 181 (2000).
[2] M. Milun, P. Pervan, and D. P. Woodruff, Rep. Prog. Phys. **65**, 99 (2002).
[3] N. J. Speer, S.-J. Tang, T. Miller, and T. C. Chiang, Science **314**, 804 (2006).
[4] P. S. Kirchman, L. Rettig, X. Zubizarreta, and V. M. Silkin, Nature Phys. **6**, 782 (2010).
[5] M. C. Yang, C. L. Lin, W. B. Su, S. P. Lin, S. M. Lu, H. Y. Lin, C. S. Chang, W. K. Hsu, and T. T. Tsong, Phys. Rev. Lett. **102**, 196102 (2009).
[6] W. B. Su, C. S. Chang, and T. T. Tsong, J. Phys. D: Appl. Phys. **43**, 013001 (2010).
[7] J. E. Ortega, F. J. Himpsel, G. J. Mankey, and R. F. Willis, Phys. Rev. B **47**, 1540 (1993).
[8] J. J. Pagel, T. Miller, and T.-C. Chiang, Science **283**, 1709 (1999).
[9] J. E. Ortega, F. J. Himpsel, G. J. Mankey, and R. F. Willis, Surf. Rev. Lett. **4**, 361 (1997).
[10] C. M. Wei and M. Y. Chou, Phys. Rev. B **66**, 233408 (2002).
[11] S. Pan, Q. Liu, F. Ming, K. Wang, and X. Xiao, J. Phys.: Condens. Mater. **23**, 485001 (2011).
[12] N. V. Smith, N. B. Brookes, Y. Chang, and P. D. Johnson, Phys. Rev. B **49**, 332 (1994).
[13] K. Yoshimatsu, K. Horiba, H. Kumigashira, T. Yoshida, A. Fujimori, and M. Oshima, Science **333**, 319 (2011).
[14] A. F. Santander-Syro, O. Copie, T. Kondo, F. Fortuna, S. Pailhés, R. Weht, X. G. Qiu, F. Bertran, A. Nicolaou, A. Taleb-Ibrahimi, P. Le Févre, G. Herranz, M. Bibes, N. Reyren, Y. Apertet, P. Lecoeur, A. Barthélémy, and M. J. Rozenberg, Nature (London) **469**, 189 (2011).

[15]W. Meevasana, P. D. C. King, R. H. He, S-K. Mo, M. Hashimoto, A. Tamai, P. Songsiriritthigul, F. Baumberger, and Z-X. Shen, Nat. Mater. **10**, 114 (2011).

[16]P. D. C. King, R. H. He, T. Eknapakul, P. Buaphet, S.-K. Mo, Y. Kaneko, S. Harashima, Y. Hikita, M. S. Bahramy, C. Bell, Z. Hussain, Y. Tokura, Z.-X. Shen, H. Y. Hwang, F. Baumberger, and W. Meevasana, Phys. Rev. Lett. **108**, 117602 (2012).

[17]J. Mannhart and D. G. Schlom, Science **26**, 1607 (2010).

[18]H. Y. Hwang, Y. Iwasa, M. Kawasaki, B. Keimer, N. Nagaosa, and Y. Tokura, Nat. Mater. **11**, 103 (2012).

[19]K. Yoshimatsu, T. Okabe, H. Kumigashira, S. Okamoto, S. Aizaki, A. Fujimori, and M. Oshima, Phys. Rev. Lett. **104**, 147601 (2010).

[20]M. Takizawa, K. Maekawa, H. Wadati, T. Yoshida, A. Fujimori, H. Kumigashira, and M. Oshima, Phys. Rev. B **79**, 113103 (2009).

[21]T. Yoshida, M. Hashimoto, T. Takizawa, A. Fujimori, M. Kubota, K. Ono, and H. Eisaki, Phys. Rev. B **82**, 085119 (2010).

[22]S. Aizaki, T. Yoshida, K. Yoshimatsu, M. Takizawa, M. Minohara, S. Ideta, A. Fujimori, K. Gupta, P. Mahadevan, K. Horiba, H. Kumigashira, and M. Oshima, Phys. Rev. Lett. **109**, 056401 (2012).

[23]The experimental data points around the binding energy of 500 meV (bottom of the V 3*d* conduction band) were eliminated for the linear fitting because they have considerably larger error bars. This is simply because the uncertainty of the energy position results in a larger error in the momentum in the case of a band with smaller value of $|\frac{d^2E}{dk^2}|$.[11]

[24]M. Minohara, I. Ohkubo, H. Kumigashira, and M. Oshima, Appl. Phys. Lett. **90**, 132123 (2007).

[25]K. Morito, T. Suzuki, S. Sekiguchi, H. Okushi, and M. Fujimoto, Jpn. J. Appl. Phys. **39**, 166 (2000).

[26]K. A. Müller and H. Burkard, Phys. Rev. B **19**, 3593 (1979).

[27]H.-C. Li, W. Si, A. D. West, and X. X. Xi, Appl. Phys. Lett. **73**, 464 (1998).

[28]A. A. Sirenko, C. Bernhard, A. Golnik, A. M. Ckark, J. Hao, W. Si, and X. X. Xi, Nature (London) **404**, 373 (2000).

[29]S. M. Sze and K. K. Ng, *Physics of Semiconductor Devices*, 3rd ed. (Wiley, Hoboken, NJ, 2007).